Electronic Supplementary Material (ESI) for Physical Chemistry Chemical Physics.

Supplementary Information

Plastic Crystal-based Electrolytes Using Novel Dicationic Salts

Shanika Abeysooriya*[a], Minjae Lee [b] Luke A. O'Dell [c] and Jennifer M. Pringle*[a]

[a] Institute for Frontier Materials (IFM), Deakin University, Burwood Hwy, VIC 3125, Australia

[b] Department of Chemistry, Kunsan National University, Gunsan, 54150, South Korea

[c] Institute for Frontier Materials, Deakin University, Geelong VIC, 3220, Australia

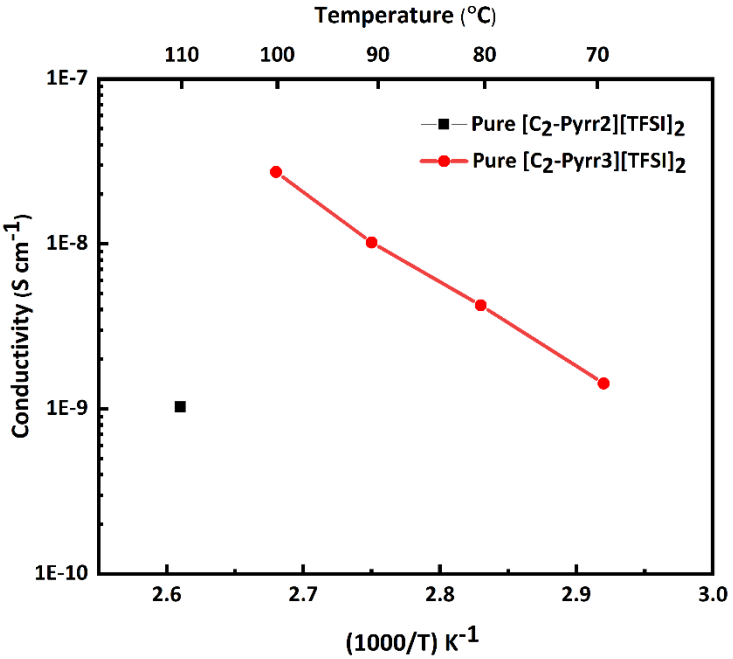

Figure S 1. Arrhenius plot of conductivity for neat $[C_2\text{-Pyrr2}][TFSI]_2$ and neat $[C_2\text{-Pyrr3}][TFSI]_2$.

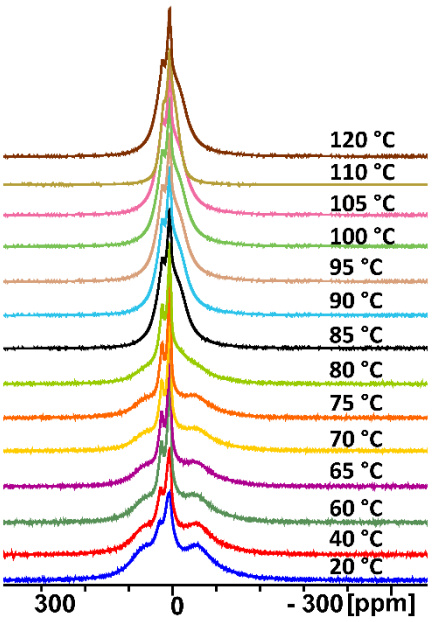

Figure S 2. ^1H static NMR of neat $[C_2\text{-Pyrr2}][TFSI]_2$

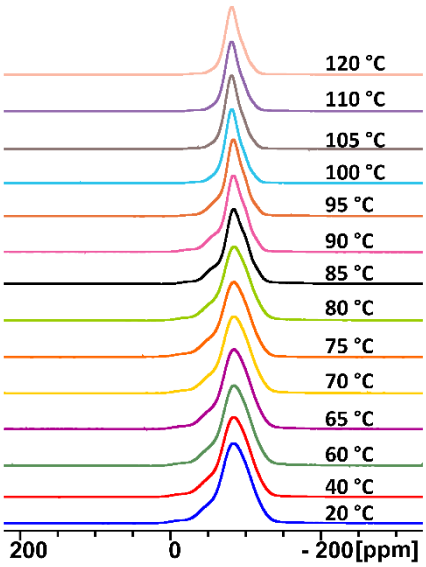

Figure S 3. ^{19}F static NMR of neat $[C_2\text{-Pyrr2}][TFSI]_2$

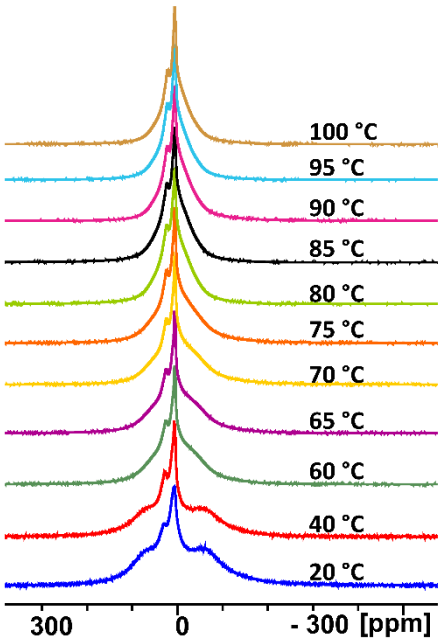

Figure S 4. ^{1}H static NMR of neat $[C_2\text{-Pyrr3}][TFSI]_2$

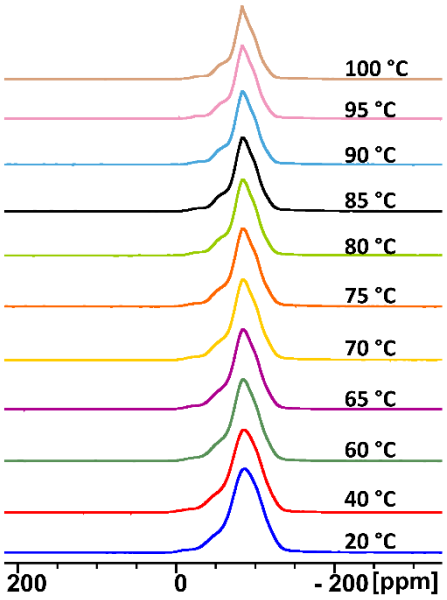

Figure S 5. ^{19}F static NMR of neat $[C_2\text{-Pyrr3}][TFSI]_2$

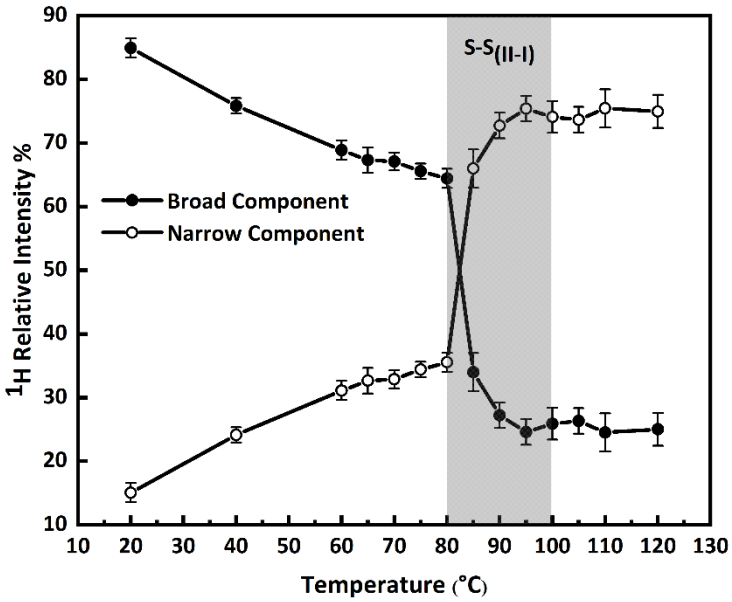

Figure S 6. ^{1}H NMR relative intensity of neat $[C_2\text{-Pyrr2}][TFSI]_2$ recorded at increasing temperatures. The phase II to II transition is marked with a shaded area.

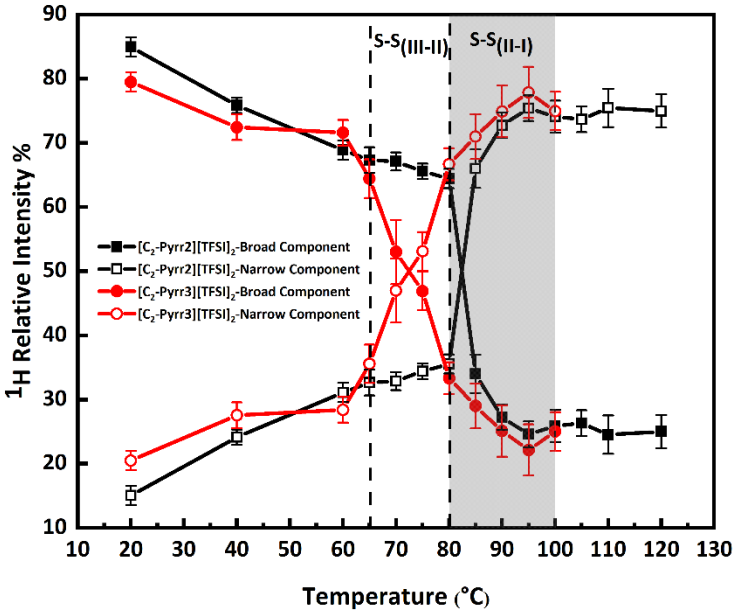

Figure S 7. ^{1}H NMR relative intensity of neat $[C_2\text{-Pyrr2}][TFSI]_2$ and of neat $[C_2\text{-Pyrr3}][TFSI]_2$ recorded at increasing temperatures. The III to II phase transition of pure $[C_2\text{-Pyrr3}][TFSI]_2$ is shown by the clear region and the II to I phase transition of each system marked by the shaded region.

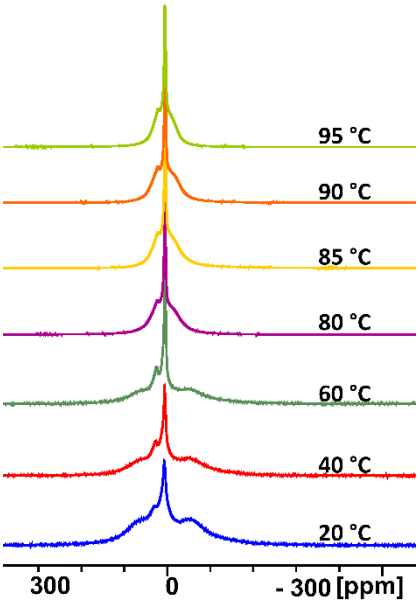

Figure S 8. ^{1}H static NMR of $[C_2\text{-Pyrr2}][TFSI]_2$/LiTFSI (10 mol % LiTFSI).

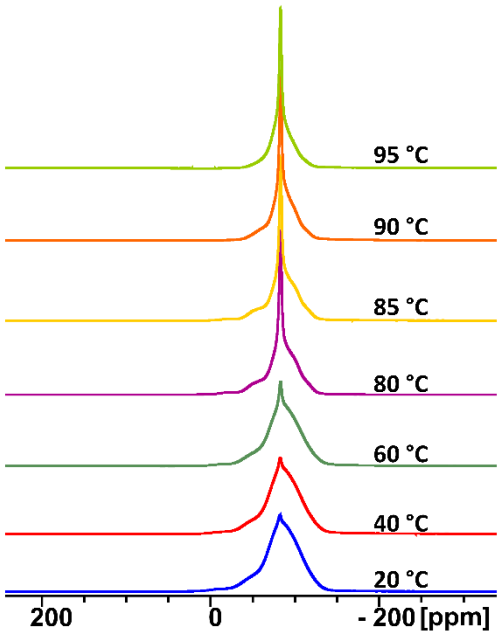

Figure S 9. ^{19}F static NMR of $[C_2\text{-Pyrr2}][TFSI]_2$/LiTFSI (10 mol % LiTFSI).

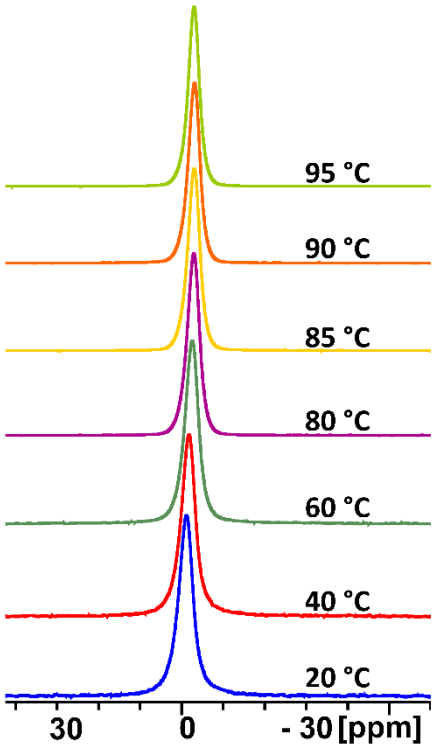

Figure S 10. ^{7}Li static NMR of $[C_2\text{-Pyrr2}][TFSI]_2$/LiTFSI (10 mol % LiTFSI).

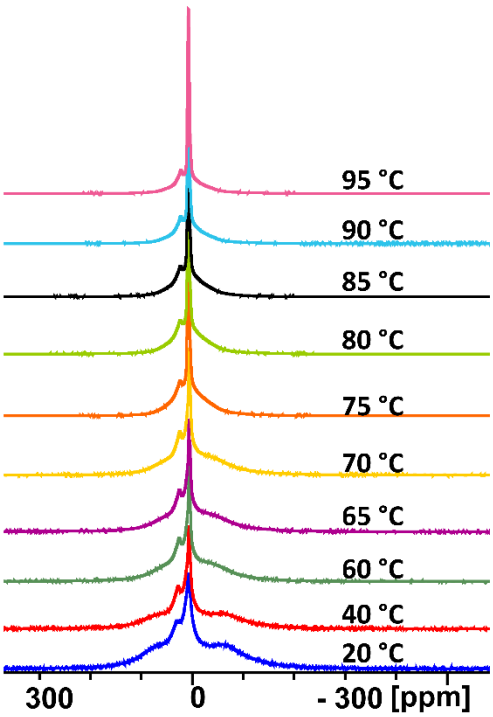

Figure S 11. ^{1}H static NMR of $[C_2\text{-Pyrr3}][TFSI]_2$/LiTFSI (10 mol % LiTFSI).

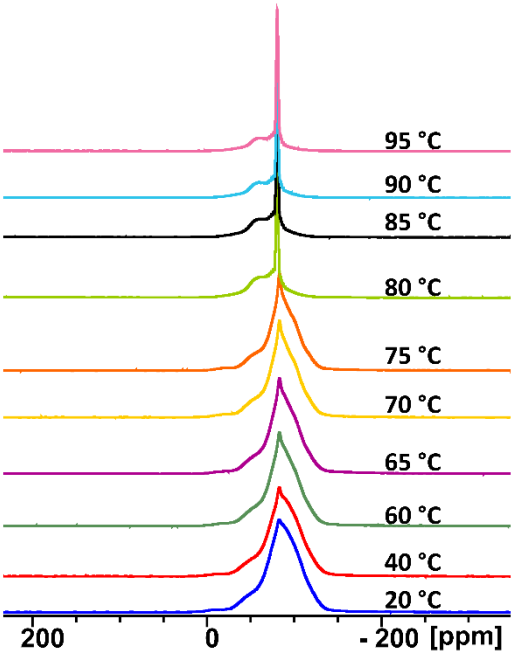

Figure S 12. ^{19}F static NMR of $[C_2\text{-Pyrr3}][TFSI]_2$/LiTFSI (10 mol % LiTFSI).

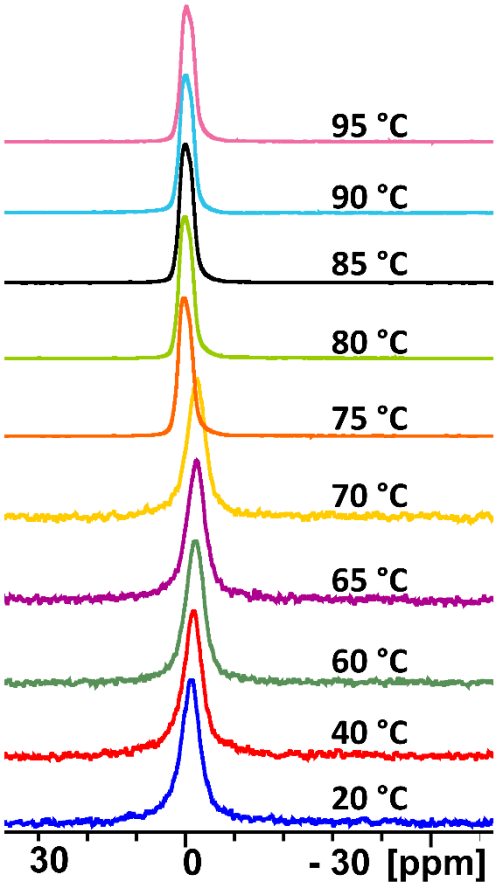

Figure S 13. ^{7}Li static NMR of [C_2-Pyrr3][TFSI]$_2$/LiTFSI (10 mol % LiTFSI).

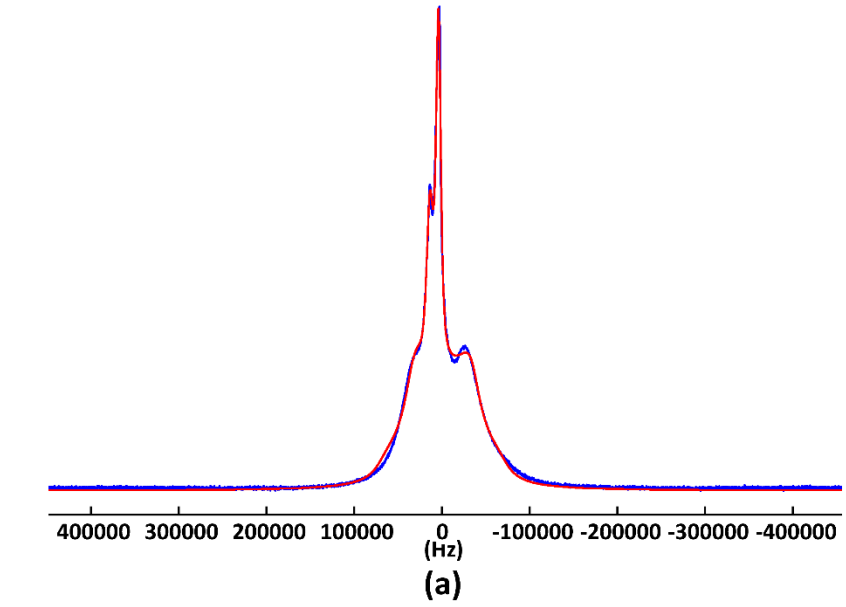

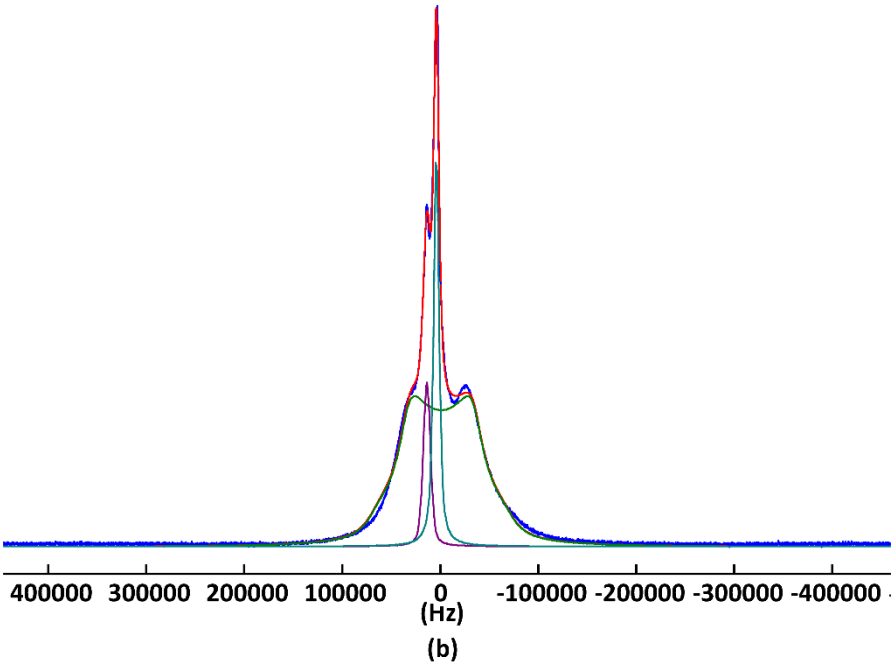

Figure S 14. (a) and (b) ^{1}H static NMR fitting using DMFIT software.

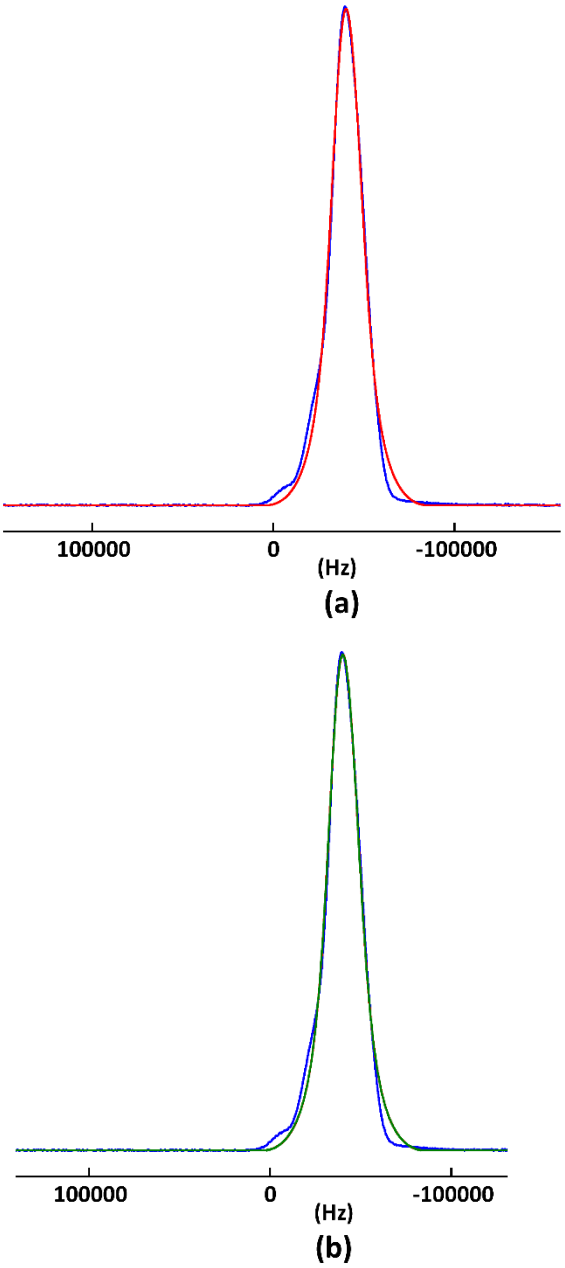

Figure S 15. (a) and (b) ^{19}F static NMR fitting using DMFIT software.

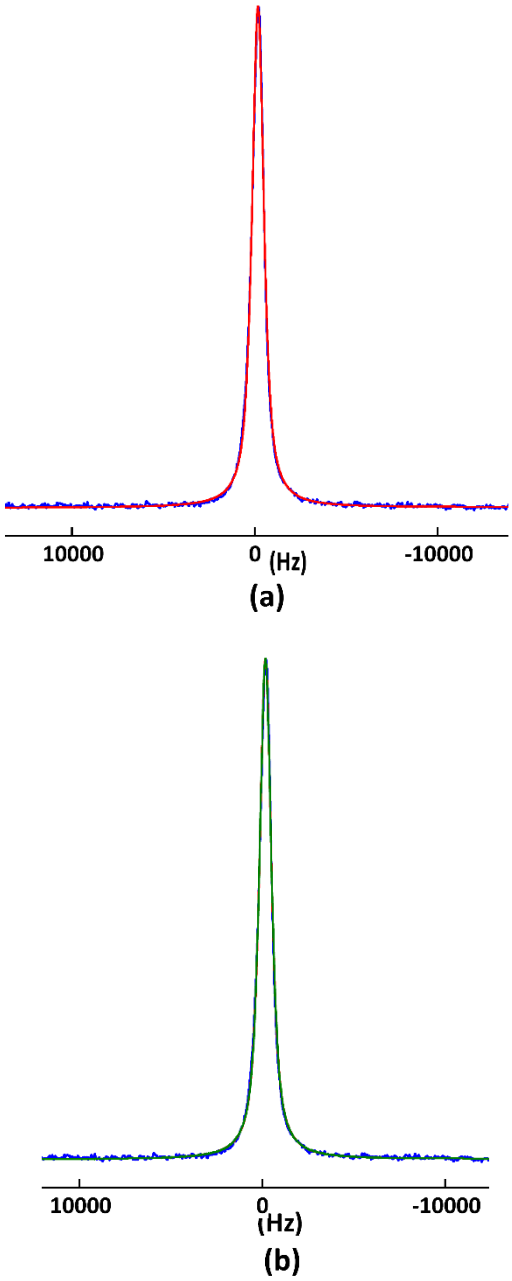

Figure S 16. (a) and (b) ^{7}Li static NMR fitting using DMFIT software.

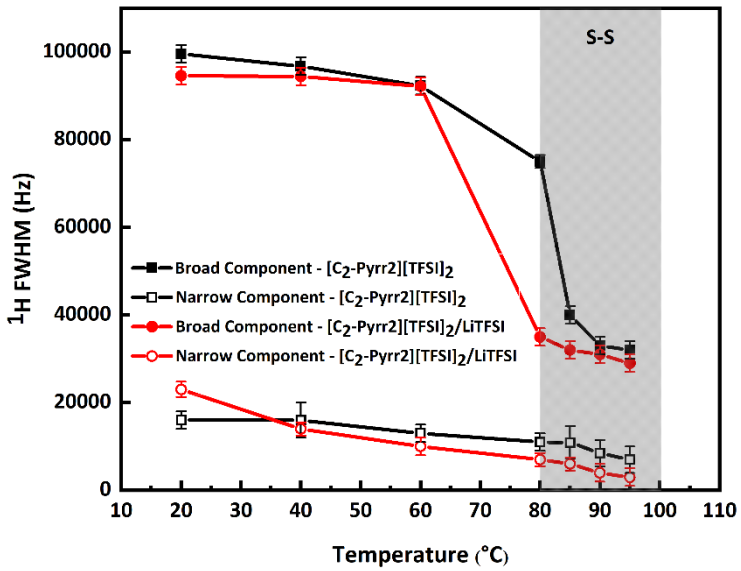

Figure S 17. ^{1}H NMR line widths of pure [C_2-Pyrr2][TFSI]$_2$ and [C_2-Pyrr2][TFSI]$_2$/LiTFSI (10 mol % LiTFSI) mixture recorded at increasing temperatures. The phase transition of both pure [C_2-Pyrr2][TFSI]$_2$ (80–100 °C) and [C_2-Pyrr2][TFSI]$_2$/LiTFSI is marked with a shaded area.

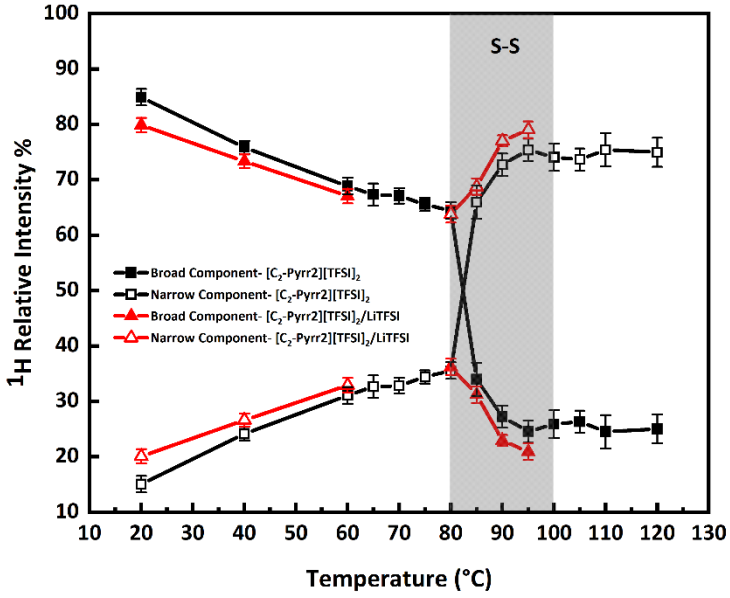

Figure S 18. ^{1}H NMR relative intensity of pure [C_2-Pyrr2][TFSI]$_2$ and [C_2-Pyrr2][TFSI]$_2$/LiTFSI (10 mol% LiTFSI) mixture recorded at increasing temperatures. The phase transition of both pure [C_2-Pyrr2][TFSI]$_2$ (80–100 °C) and [C_2-Pyrr2][TFSI]$_2$/LiTFSI is marked with a shaded area.

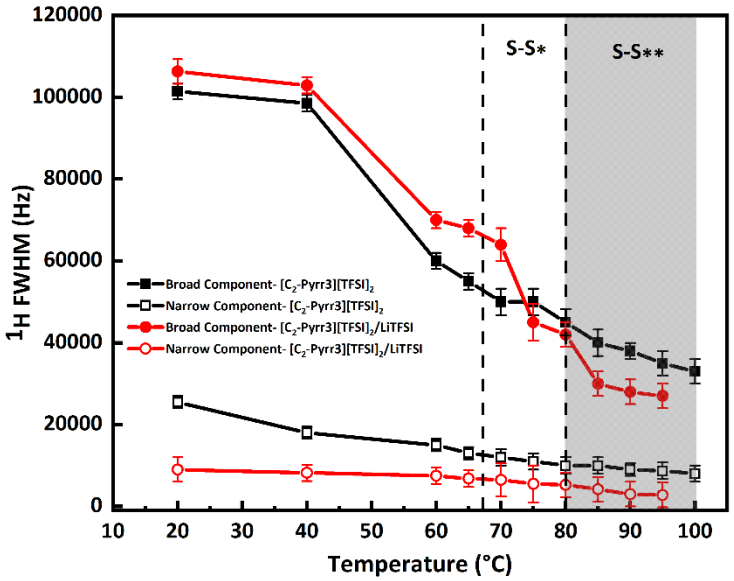

Figure S 19. ^{1}H NMR line widths of [C_2-Pyrr3][TFSI]$_2$/LiTFSI (10 mol % LiTFSI) recorded at increasing temperatures. The phase transition for both pure [C_2-Pyrr3][TFSI]$_2$ and [C_2-Pyrr3][TFSI]$_2$/LiTFSI is shown as S*: 65–80 °C and S**: 80–100 °C.

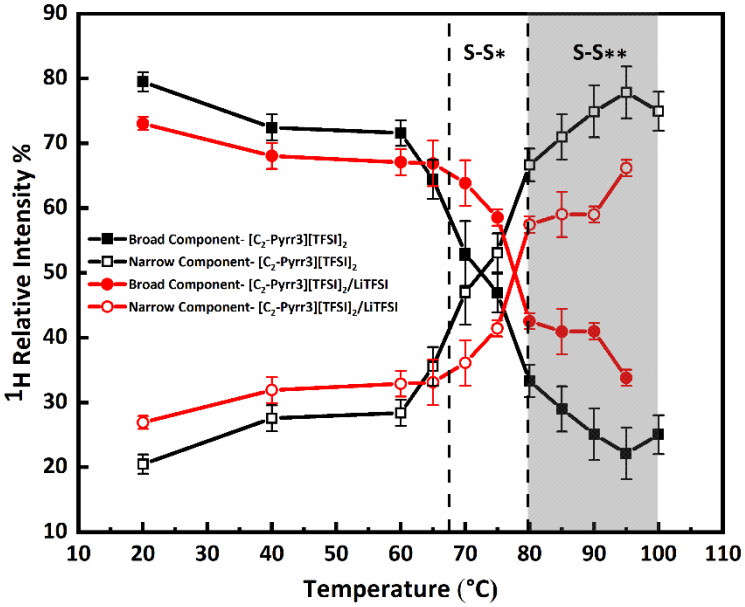

Figure S 20. ^{1}H NMR relative intensity of [C_2-Pyrr3][TFSI]$_2$/LiTFSI (10 mol % LiTFSI) recorded at increasing temperatures. The phase transition for both pure [C_2-Pyrr3][TFSI]$_2$ and [C_2-Pyrr3][TFSI]$_2$/LiTFSI is shown as S*: 65–80 °C and S**: 80–100 °C.

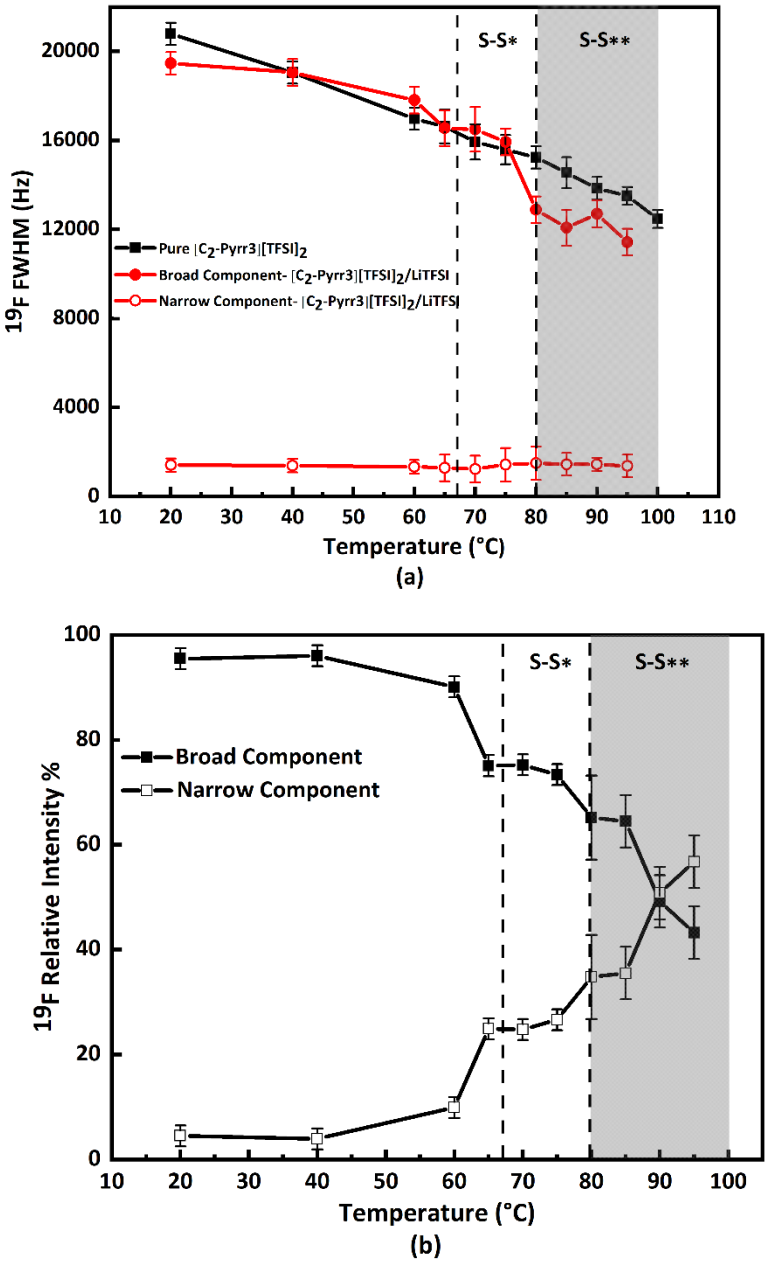

Figure S 21. (a) ^{19}F NMR line width of pure [C_2-Pyrr3][TFSI]$_2$ and [C_2-Pyrr3][TFSI]$_2$/LiTFSI (10 mol % LiTFSI) and (b) ^{19}F NMR relative intensity of [C_2-Pyrr3][TFSI]$_2$/LiTFSI (10 mol % LiTFSI) recorded at increasing temperatures. The phase transition for both pure pure [C_2-Pyrr3][TFSI]$_2$ and [C_2-Pyrr3][TFSI]$_2$/LiTFSI is shown as S_*: 65–80 °C and S_{**}: 80–100 °C. For FWHM and relative intensity analysis, CSA model and a Gaussian model (for the narrow component) were used in combination for peak fitting.

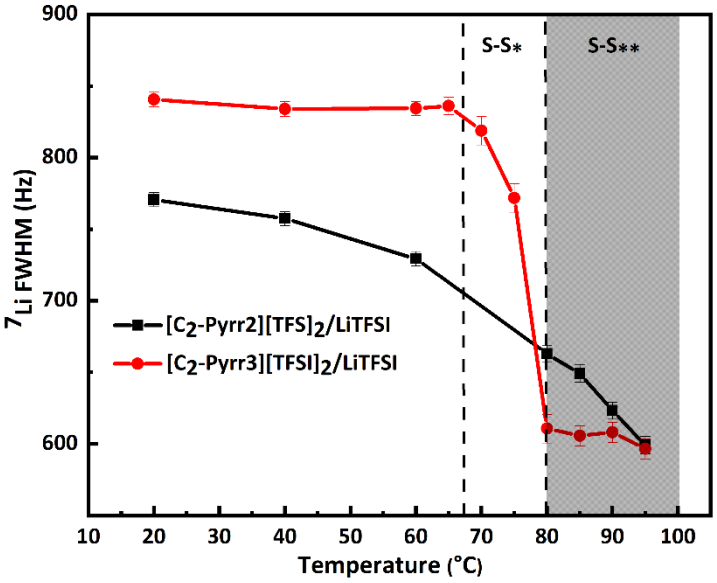

Figure S 22. ^{7}LiNMR line widths of $[C_2\text{-Pyrr2}][TFSI]_2$/LiTFSI and $[C_2\text{-Pyrr3}][TFSI]_2$/LiTFSI recorded at increasing temperatures. The 68–80 °C phase transition of $[C_2\text{-Pyrr3}][TFSI]_2$/LiTFSI is shown by the clear region and the 80–100 °C phase transition of each system marked as the shaded region.